The Conformation of Cytochalasin D in DMSO Solution from ^1H and ^{13}C NMR Relaxation Rates

Antonella Maccotta,[a] Gianni Valensin,[b] Nicola Gaggelli[b] and Elena Gaggelli[b]
[a] *Department of Chemistry, University of Basilicata, Potenza 85100, Italy*
[b] *Department of Chemistry, University of Siena, Siena 53100, Italy*

The conformation of cytochalasin D in solution has been delineated by measuring ^{13}C and ^1H NMR spin–lattice relaxation rates and NOESY spectra. The motional correlation time was evaluated at 0.26 ns at 300 K. A comparison with the structure of cytochalasin B in the same solvent discloses several similarities, except for a small distortion of the five-membered ring. The difference in activity is therefore ascribed to the different hydrophobicity of substituents within the macrocycle.

The cytochalasins are a group of natural metabolic products of phytopathogenic fungi.[1] They interfere with several cellular motile functions such as endocytosis, cell movement, and pseudopod extension and retraction.[1] Among the several examples isolated and characterized, only cytochalasin B (CB) has been shown to act as a specific and potent inhibitor of D-glucose transport in human erythrocytes.[2] The conformational features of CB have been studied by X-ray[3] and NMR[4,5] methods. For CB in [$^2H_6$]DMSO solution, the whole molecule was shown to reorient in a nearly isotropic fashion (τ_c = 0.21 ns at 298 K) with few degrees of internal motional flexibility.[5] Calculated proton–proton distances indicated (i) distorted boat conformation of the six-membered ring, (ii) planar conformation of the five-membered ring, (iii) g^- conformation at the point of attachment of the phenyl ring and (iv) parallelism between the phenyl ring and the macrocycle which showed flatness at the level of the C_{20}–C_{23} portion.[5] Solid state and solution structures were therefore found to be very similar; on this basis a mechanism was suggested for the inhibitory activity involving hydrogen bonds with the glucose carrier.

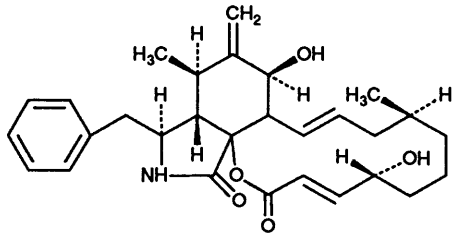

Cytochalasin B

Here we present NMR data on cytochalasin D (CD) (Fig. 1) with the aim of delineating the structure in solution of this inactive metabolite so that a comparison to the solid-state structure[3] and with solution and crystal structures of CB can be carried out.

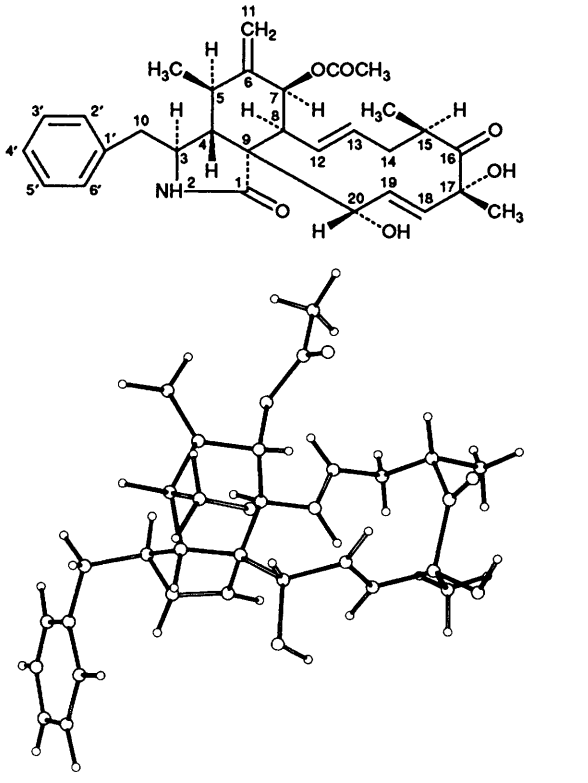

Fig. 1 Molecular formula of cytochalasin D and the 'preferred' conformation in solution as obtained by projecting the molecular model obtained with the Macromodel software

Experimental

Cytochalasin D was supplied by Sigma Chemical Co. and used without further purification. Solutions were made in [$^2H_6$]-DMSO 99.95% (Merck) and carefully degassed by bubbling nitrogen gas.

NMR experiments were carried out on Bruker FT-NMR spectrometers at 7.05 and 14.11 T at the constant temperature of 300 ± 1 K. Chemical shifts were referenced to internal TMS. ^{13}C–^1H 2D heterocorrelated spectra were obtained by using the procedure described in ref. 6. Double-quantum filtered ^1H–^1H COSY spectra were obtained by using the pulse sequence described in ref. 7. ^1H–^1H NOESY experiments were carried out at different values of the mixing time with the pulse sequence described in ref. 8. Cross-peak intensities were measured by taking ratios between the cross-peak volumes in the 2D map at any value of the mixing time and the corresponding diagonal peak volumes at zero mixing time.

^{13}C and ^1H spin–lattice relaxation rates were measured with inversion recovery pulse sequences and calculated with exponential regression analysis of the recovery curves of longitudinal magnetization components.

Results and Discussion

^{13}C and ^1H assignments, reported in Table 1, were facilitated by the use of ^{13}C–^1H 2D heterocorrelation spectroscopy and ^1H–^1H double-quantum filtered COSY (Fig. 2). The ^{13}C resonances were assigned by comparison with data in the literature

Table 1 75.4 MHz ^{13}C NMR and 300 MHz ^{1}H NMR chemical shifts and spin–lattice relaxation rates for cytochalasin D (50 mmol dm^{-3} in $[^2H_6]$DMSO at T = 300 K)

Carbon	δ	^{13}C R_1/s^{-1}	Proton	δ	^{1}H R_1/s^{-1}	^{1}H R_{1l}*/s^{-1}
C_1	170.0	0.64 ± 0.02				
			H_2	8.08	0.63 ± 0.02	0.50
C_3	52.5	5.60 ± 0.25	H_3	3.08	1.64 ± 0.10	1.40
C_4	47.5	4.35 ± 0.16	H_4	1.96	2.51 ± 0.14	2.42
C_5	37.8	4.20 ± 0.18	H_5	2.46	1.32 ± 0.05	1.25
$CH_3(5)$	12.8	2.78 ± 0.11	$CH_3(5)$	0.38	5.41 ± 0.21	
C_6	150.7	1.16 ± 0.41				
C_7	70.2	4.17 ± 0.17	H_7	3.54	1.81 ± 0.08	
C_8	46.1	5.56 ± 0.23	H_8	2.67	3.12 ± 0.14	
C_9	53.1	0.38 ± 0.01				
C_{10}	43.6	9.09 ± 0.35	H_{10a}	2.78	5.56 ± 0.19	
			H_{10b}	2.53	3.13 ± 0.11	
$C_{1'}$	137.0	0.64 ± 0.02				
$C_{2'}$, $C_{6'}$	129.6	3.70 ± 0.16	$H_{2'}$, $H_{6'}$	7.13	0.83 ± 0.04	0.72
$C_{3'}$, $C_{5'}$	128.3	4.17 ± 0.11	$H_{3'}$, $H_{5'}$	7.28	1.50 ± 0.06	1.44
$C_{4'}$	126.4	5.00 ± 0.14	$H_{4'}$	7.20	1.48 ± 0.06	1.44
C_{11}	111.4	9.01 ± 0.29	H_{11a}	4.99	3.33 ± 0.15	
			H_{11b}	4.77	3.85 ± 0.15	
C_{12}	130.8	5.50 ± 0.19	H_{12}	5.39	1.50 ± 0.04	
C_{13}	131.6	5.48 ± 0.20	H_{13}	5.06	1.32 ± 0.06	1.26
C_{14}	31.5	9.12 ± 0.34	H_{14a}	2.15	5.00 ± 0.21	4.83
			H_{14b}	1.88	6.90 ± 0.28	6.75
C_{15}	41.4	5.52 ± 0.18	H_{15}	2.73	4.55 ± 0.25	4.42
$CH_3(15)$	19.2	2.86 ± 0.13	$CH_3(15)$	1.04	3.12 ± 0.13	
C_{16}	173.5	0.32 ± 0.02				
C_{17}	77.4	0.42 ± 0.01				
$CH_3(17)$	24.6	3.33 ± 0.09	$CH_3(17)$	1.38	3.57 ± 0.15	
			OH(17)	4.56	0.74 ± 0.03	
C_{18}	127.0	5.56 ± 0.15	N_{18}	5.11	2.52 ± 0.06	2.37
C_{19}	132.1	5.20 ± 0.11	H_{19}	5.85	1.14 ± 0.06	1.24
C_{20}	76.4	7.14 ± 0.23	H_{20}	5.25	2.17 ± 0.10	2.28
			OH(20)	4.94	1.59 ± 0.08	
C_{21}	210.2	0.24 ± 0.01				
C_{22}	20.8	1.84 ± 0.08	H_{22}	2.28	1.01 ± 0.04	

[a] Calculated proton spin–lattice relaxation rates. See text for details.

Table 2 Coupling constants (Hz) measured in 300 MHz ^{1}H NMR spectra of cytochalasin D (50 mmol dm^{-3} in $[^2H_6]$DMSO at T = 300 K)

Proton	Observed couplings
H_3	H_4 (2.8); H_{10a} (4.6); H_{10b} (9.2)
H_4	N_3 (2.8); H_5 (5.8)
H_5	H_4 (5.8)
H_7	H_8 (9.7)
H_8	H_7 (9.7); H_{12} (9.7)
H_{10a}	H_3 (4.6); H_{10b} (13.8);
H_{10b}	H_3 (9.2); H_{10a} (13.8)
H_{12}	H_8 (9.7); H_{13} (15.4)
H_{13}	H_{12} (15.4); H_{14a} (13.0); H_{14b} (4.6)
H_{14a}	H_{13} (13.0); H_{14b} (13.8); H_{15} (12.0)
H_{14b}	H_{13} (4.6); H_{14a} (13.8); H_{15} (4.8)
H_{15}	H_{14a} (12.0); H_{14b} (4.8)
H_{18}	H_{19} (15.9); H_{20} (2.2)
H_{19}	H_{18} (15.9); H_{20} (2.4)
H_{20}	H_{18} (2.2); H_{19} (2.4)

and spectral editing; proton resonances were consequently assigned by the ^{13}C–^{1}H and ^{1}H–^{1}H scalar connectivities. In some cases comparison with NMR spectra of other cytochalasins was sufficient to assign a given resonance.

Proton–proton coupling constants (listed in Table 2) were directly calculated from the 1D and the COSY spectra and ratified with the aid of selective spin decoupling experiments. J Values contain, in principle, information about the torsional arrangement of adjacent protons, but unequivocal delineation of conformation within the macrocyclic ring was not possible because of the double maxima of the angular dependence of ^{3}J and also of difficulties in accounting for substituent electronegativity effects in the Karplus equation. However the very large couplings measured for some proton pairs indicate that conformational inversion does not occur.

The same goal was better accomplished by measuring dipolar cross-relaxation rates in NOESY experiments and, then, by simulating the proton spin–lattice relaxation rates. The intensity of any cross-peak, I_{AB}, in a NOESY experiment is a function of the mixing time t_m. An optimal value of t_m yielding maximum I_{AB} can always be found by plotting the intensity of cross-peaks, normalized to the intensity of the corresponding diagonal peak at zero-mixing time, $[I_C = I_{AB}(t_m)/I_{AA}(t_m = 0)]$, against t_m. Typical plots are shown in Fig. 3 for three cross-peaks detected in the NOESY spectrum of CD in $[^2H_6]$DMSO, namely the cross-peaks corresponding to the H_{12a}–H_{12b}, H_4–H_{20} and H_{19}–H_{20} dipolar interactions. The same behaviour, with a maximum centred at t_m *ca.* 300 ms, was observed for all the cross-peaks, suggesting that all proton–proton internuclear vectors experience the same modulation frequencies from reorientational motions.[8] From the cross-peak intensities, distances can be evaluated by making ratios to a cross-peak connecting protons at fixed distance, *e.g.* two geminal protons and using eqn. (1).

$$\frac{I_{C1}}{I_{C2}} = \left(\frac{r_2}{r_1}\right)^6 \quad (1)$$

Eqn. (1) was used under the assumptions that proton–proton dipolar interactions are not cross-correlated and that identity of internuclear vector dynamics occurs. This last assumption is supported by the apparent rigidity of the macrocycle which

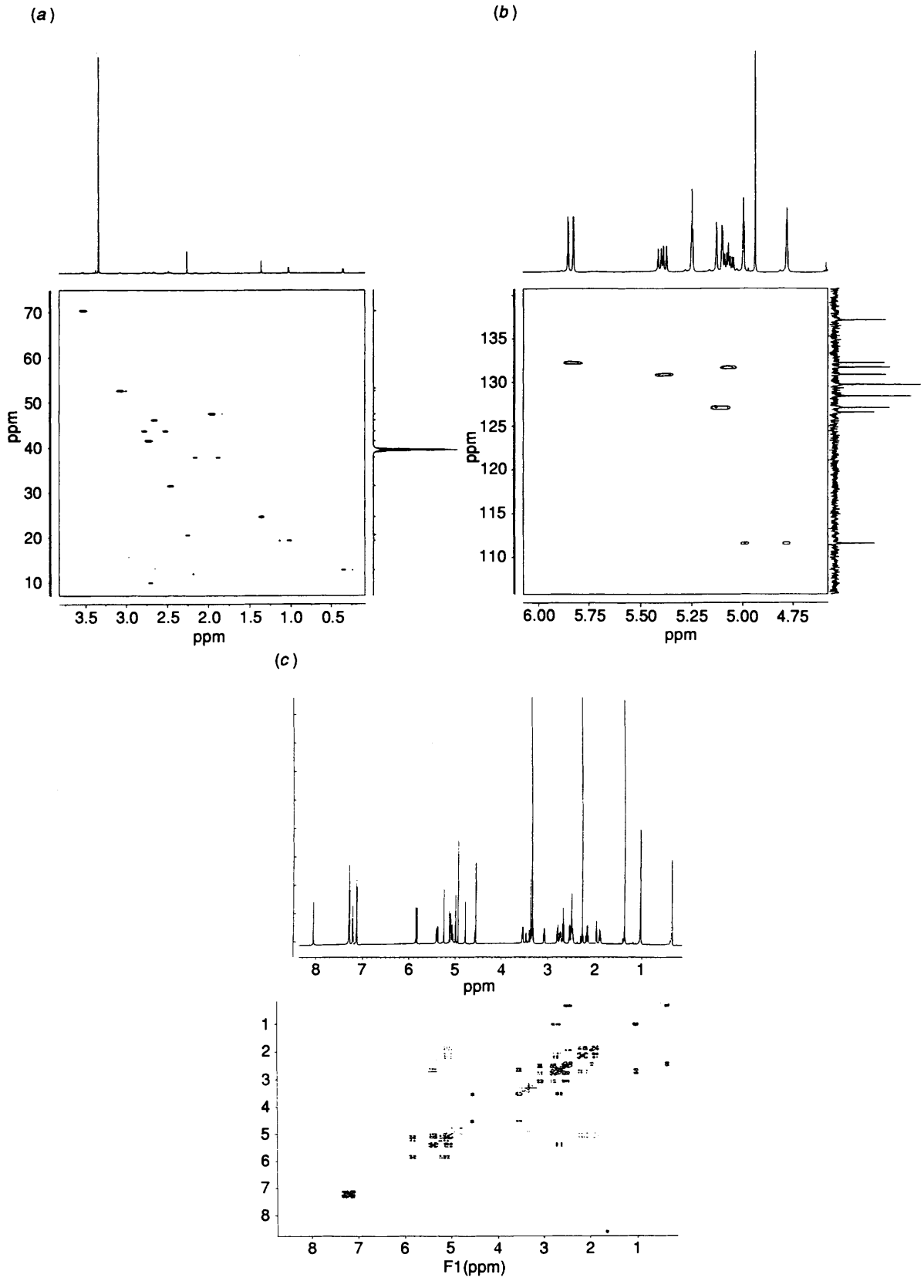

Fig. 2 (*a*) and (*b*) expanded regions of the ^{13}C–^{1}H chemical shift correlated 2D spectrum and (*c*) double quantum filtered ^{1}H–^{1}H chemical shift correlated 2D spectrum obtained from cytochalasin D 50 mmol dm^{-3} in [$^{2}H_6$]DMSO at T = 300 K

reflects in coherence of ^{13}C spin–lattice relaxation rates (*vide infra*) and on the same t_m dependence of NOESY cross-peaks.

Obtained distances are reported in Table 3 and allow to gain some relevant information on geometric parameters: the dipolar interactions H_3–H_{10b}, H_5–H_{10a}, H_5–H_{10b} suggest for the six-membered and the five-membered rings distorted boat and half-chair (degree of pucker *ca.* 10°) conformations respectively, in agreement with the solid state structure; the dipolar interactions H_{20}–H_4 and H_{20}–H_{19} suggest that both H_{20} and H_{19} are axial downward; the interaction H_{19}–OH(20) locates the hydroxy

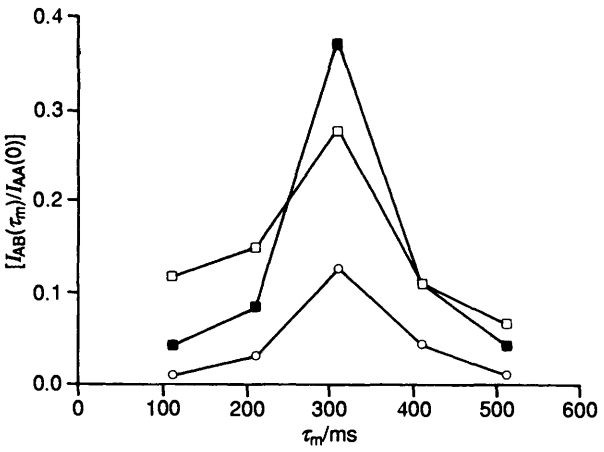

Fig. 3 Plot of some normalized cross-peak intensities *vs.* the mixing time from NOESY spectra of cytochalasin D 50 mmol dm^{-3} in [$^2H_6$]-DMSO at T = 300 K. See text for details. □, H_{20}–H_{19}; ■, H_{21}–H_{24}; ○, H_{12a}–H_{12b}.

Table 3 Cross-peak normalized intensities and proton–proton distances calculated from NOESY experiments for cytochalasin D (50 mmol dm^{-3} in [$^2H_6$]DMSO at T = 300 K)

Proton pair	I_C[a]	r[b]/Å
H_{19}–H_{20}	0.088 ± 0.009	2.1_5
H_3–H_{10b}	0.037 ± 0.004	2.5
H_4–H_{20}	0.119 ± 0.020	2.0_5
H_{11a}–H_{11b}	0.365 ± 0.034	1.7
H_{10a}–H_{10b}	0.278 ± 0.026	1.8[c]
H_{14a}–H_{14b}	0.284 ± 0.030	1.8[c]
H_5–H_{10a}	0.239 ± 0.025	1.9
H_5–H_{10b}	0.076 ± 0.007	2.3
H_{19}–OH(20)	0.031 ± 0.003	2.7

[a] Calculated at 300 ms mixing time; see text for details. [b] only the first decimal figure is given since the error has been evaluated at *ca.* 2%. [c] Taken as the reference distance.

proton in the equatorial plane. It is relevant to note that all the detected features agree with the calculated size of coupling constants.

The final conformation, shown in Fig. 1 as a computer simulated molecular model, was obtained by simulating the experimental relaxation rates of the macrocycle protons with eqn. (2)[9]

$$R_i = \sum_{j \neq i} \rho_{ij} + \sum_{j \neq i} \sigma_{ij} = \frac{1}{10}\gamma_H^4 h^2 \left\{ \frac{3\tau}{1 + \omega^2\tau^2} + \frac{12\tau}{1 + 4\omega^2\tau^2} \right\} \sum_{j \neq i} r_{ij}^{-6} \quad (2)$$

where h is the reduced Planck constant ($= h/2\pi$), γ_H the magnetogyric ratio, ω the proton Larmor frequency, τ the correlation time and r_{ij} the distance between H_i and H_j. R_i values were simulated by assuming (i) τ = 0.26 ns; (ii) absence of cross correlation and (iii) negligible contributions to R_i from mechanisms other than the dipolar. The value of τ = 0.26 ns was calculated from ^{13}C spin–lattice relaxation rates (Table 1). The ^{13}C–{^1H} nuclear Overhauser effects (not reported in Table 1) for all protonated carbons were found at almost their maximum value (η_{max} = 1.98), thus demonstrating that the ^{13}C–^1H dipole–dipole interaction provides the main relaxation mechanism. The spin–lattice relaxation rates could therefore be interpreted in terms of dipolar interaction terms between spin-pairs at the fixed distance of 1.09 Å[10] modulated by a nearly isotropic reorientational correlation time. It was in fact evident that all protonated carbons were relaxing with the same normalized rate constant (R_i/n_H, where n_H is the number of protons attached to carbon) as if the motion were isotropic and the CD molecule were behaving like a spherical body. As a consequence the reorientational correlation time was calculated at 0.26 ± 0.06 ns at 300 K from the average value of normalized rates of all protonated carbons.[10,11] The only considered exception was that of *ortho* and *meta* aromatic carbons where an internal librational motion was considered to account for reduction of the spin–lattice relaxation rate in respect of the *para* carbon. By applying the model of Woessner for a C-H vector undergoing internal motion around an axis reorienting isotropically and making an angle of 60° with that vector, the correlation time for librational motion was calculated at τ_G = 0.08 ns.[11,12]

The agreement between the rates calculated in this way and the experimental rates (Table 1) was satisfactory and enabled the following final conformational assignments:

(i) The conformation around the C_{13}–C_{14} bond is such that H_{13} (perpendicular to the average macrocycle plane) is gauche to H_{14b} and trans to H_{14a}; whereas around the C_{14}–C_{15} bond H_{15} is gauche to H_{14a} and trans to H_{14b}.

(ii) As a consequence the C_{16} carbonyl lies in a plane perpendicular to the average molecular plane and the oxygen of the hydroxy at C_{17} is equatorial.

Comparison with the structure of cytochalasin B in the same solvent[4,5] discloses substantial similarity except for a small distortion of the five-membered ring: the main features of flat macrocycle portions and parallel phenyl and macrocycle rings are maintained. This suggests that the difference in activity must arise from the different hydrophobicity of substituents within the macrocycle.

Acknowledgements

The NMR spectra at 14.1 T were carried out at the NMR Service of the University of Florence. We acknowledge the director of the NMR Service, Prof. I. Bertini, for the access to the NMR facilities and Mr. M. Lucci for technical assistance.

References

1 S. W. Tannebaum, *Cytochalasins: Biochemical and Cell Biological Aspects*, Elsevier, Amsterdam, 1978.
2 C. Y. Jung and A. L. Rampal, *J. Biol. Chem.*, 1977, **252**, 5456.
3 J. F. Griffin, A. L. Rampal and C. Y. Jung, *Proc. Natl. Acad. Sci. USA*, 1982, **79**, 3759.
4 D. W. Graden and D. G. Lynn, *J. Am. Chem. Soc.*, 1984, **106**, 1119.
5 E. Gaggelli, A. Maccotta, A. Scopa and G. Valensin, *Biophys. Chem.*, 1988, **32**, 297.
6 A. Bax and G. Morris, *J. Magn. Reson.*, 1981, **42**, 501.
7 D. Marion and K. Wüthrich, *Biochem. Biophys. Res. Commun.*, 1983, **113**, 967.
8 J. Jeener, B. H. Meier, P. Bachmann and R. R. Ernst, *J. Chem. Phys.*, 1979, **71**, 4546.
9 K. Akasaka, S. Shibata, T. Imito and H. Hatano, *J. Magn. Reson.*, 1975, **17**, 413.
10 K. Dill and A. Allerhand, *J. Am. Chem. Soc.*, 1979, **101**, 4376.
11 A. Allerhand, D. Doddrell and R. Komoroski, *J. Chem. Phys.*, 1971, **55**, 189.
12 D. E. Woessner, *J. Chem. Phys.*, 1962, **36**, 1.

Paper 2/05537F
Received 16*th October* 1992
Accepted 5*th January* 1993